BIOCHEMISTRY
including biophysical chemistry & molecular biology

Article

pubs.acs.org/biochemistry

Mode of Binding of the Cyclic Agonist Peptide TC14012 to CXCR7: Identification of Receptor and Compound Determinants

Nicolas Montpas,[†,‡] Jérôme Cabana,[§] Geneviève St-Onge,[†] Stéphanie Gravel,[†,‡] Geneviève Morin,[†] Tomoko Kuroyanagi,[∥] Pierre Lavigne,[§] Nobutaka Fujii,[∥] Shinya Oishi,[∥] and Nikolaus Heveker*[,†,‡]

[†]Research Centre, Sainte-Justine Hospital, University of Montreal, Montréal H3T 1C5, Canada

[‡]Department of Biochemistry, University of Montreal, Montréal H3T 1J4, Canada

[§]Departments of Biochemistry and Pharmacology, University of Sherbrooke, Sherbrooke J1H 5N4, Canada

[∥]Graduate School of Pharmaceutical Sciences, Kyoto University, Sakyo-ku, Kyoto 606-8501, Japan

Supporting Information

ABSTRACT: The chemokine receptor CXCR7 is an atypical CXCL12 receptor that, as opposed to the classical CXCL12 receptor CXCR4, signals preferentially via the β-arrestin pathway and does not mediate chemotaxis. We previously reported that the cyclic peptide TC14012, a potent CXCR4 antagonist, also engaged CXCR7, albeit with lower potency. Surprisingly, the compound activated the CXCR7−arrestin pathway. The reason underlying the opposite effects of TC14012 on CXCR4 and CXCR7, and the mode of binding of TC14012 to CXCR7, remained unclear. The mode of binding of TC14012 to CXCR4 is known from cocrystallization of its analogue CVX15 with CXCR4. We here report the the mode of binding of TC14012 to CXCR7 by combining the use of compound analogues, receptor mutants, and molecular modeling. We find that the mode of binding of TC14012 to CXCR7 is indeed similar to that of CVX15 to CXCR4, with compound positions Arg2 and Arg14 engaging CXCR7 key residues D179$^{4.60}$ (on the tip of transmembrane domain 4) and D275$^{6.58}$ (on the tip of transmembrane domain 6), respectively. Interestingly, the TC14012 parent compound T140 is not a CXCR7 agonist, because of conformational constraints in its pharmacophore, which in TC14012 are relieved through C-terminal amidation. However, an engineered salt bridge between the CXCR7 ECL2 substitution R197D and compound residue Arg1 permitted T140 agonism by repositioning the compound in the binding pocket. In conclusion, our results show that the opposite effect of TC14012 on CXCR4 and CXCR7 is not explained by different binding modes. Rather, engagement of the interface between transmembrane domains and extracellular loops readily triggers CXCR7, but not CXCR4, activation.

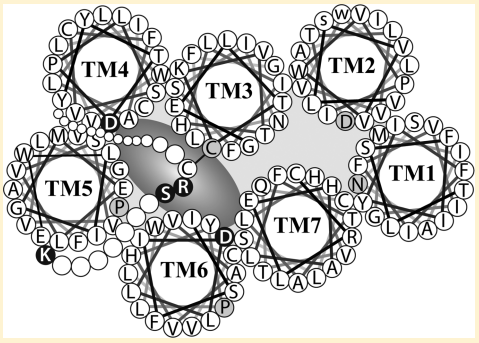

CXCR7 (also known as ACKR3) is a receptor for chemokines CXCL11 and CXCL12, which in turn also bind CXCR3 and CXCR4, respectively.[1] In contrast to these receptors, CXCR7 does not mediate chemotaxis and preferentially signals via the β-arrestin pathway.[1−3] CXCR7 is highly expressed by neovascular endothelia and many cancer cell types and has been implicated in tumor growth via direct action on cancer cells, and through a potential role in neovascularization.[1,4−6] Clinical interest of CXCR7 was recognized early on and validated by experiments in which synthetic CXCR7 ligands slowed tumor growth.[1] It subsequently turned out that these ligands, as well as all CXCR7 ligands described thereafter, acted as agonists of the arrestin pathway.[2,7−9]

Receptor determinants interacting with synthetic CXCR7 ligands have not yet been identified, but such information will be crucial for the rational design of new drug candidates targeting CXCR7. We have previously reported that the cyclic peptide TC14012, known as a potent CXCR4 antagonist, also engaged CXCR7, albeit with a much lower potency.[8] Contrary to its antagonist effect on CXCR4, it is an agonist of the CXCR7−arrestin pathway. Whether this opposite effect on the two receptors results from different modes of binding of the compound to CXCR4 and CXCR7 or from different responses of the receptor to ligands bound in a likewise manner remained unknown. The mode of binding of the compounds to CXCR4 is well-characterized, as the TC14012 analogue CVX15 has been cocrystallized with CXCR4,[10] providing detailed insight into the relevant interaction determinants. Therefore, we reasoned, TC14012 was a good starting point for the elucidation of CXCR7 interaction determinants with synthetic ligands.

We here report the mode of binding of TC14012 to CXCR7 and identify key residues in both the receptor and the compound by combining the use of compound analogues with receptor mutagenesis and molecular modeling. The interaction of TC14012 with CXCR7 is similar to that of

Received: December 16, 2014
Revised: January 30, 2015
Published: January 30, 2015

DOI: 10.1021/bi501526s
Biochemistry 2015, 54, 1505−1515

CVX15 with CXCR4: receptor key residues are CXCR7 D179$^{4.60}$ on the tip of TM4 and D275$^{6.58}$ on the tip of TM6, which engage compound positions Arg2 and Arg14, respectively. Unlike the case in CXCR4, no ionic interaction with CXCR7 extracellular loop 2 (ECL2) was identified, but substitution of the repulsive R197 in CXCR7 ECL2 with alanine (R197A) yields a receptor that is potently activated by TC14012, with an EC_{50} equal to that of the endogenous CXCL12 (14 nM) in our assay. Interestingly, the TC10412 parent compound T140 was not a CXCR7 agonist. This was due to conformational constraints in its pharmacophore, which are relieved in TC14012 by C-terminal amidation. However, introduction of a salt bridge by the CXCR7 ECL2 substitution R197D, which interacted with compound residue Arg1, repositioned T140 in the binding pocket and permitted activation of the mutant receptor.

Taken together, the study identifies key residues of CXCR7 involved in the interaction with synthetic agonists and shall guide future drug design efforts.

EXPERIMENTAL PROCEDURES

Peptide Synthesis. The peptides were synthesized according to the procedures described in our previous studies.[11,12] Briefly, the peptide sequences were synthesized by a standard protocol of Fmoc-based solid-phase peptide synthesis. The protected peptide resin was treated with a cocktail of deprotection reagents [TFA/thioanisole/*m*-cresol/EDT/H_2O (80:5:5:5:5) or TFA/EDT/H_2O/TIS (94:2.5:2.5:1)]. After removal of the resin by filtration, the crude peptide was dissolved in H_2O, and the pH was adjusted to 8.0 with NH_4OH for disulfide bond formation. The product was purified by preparative high-performance liquid chromatography on a Cosmosil 5C18-ARII preparative column (Nacalai Tesque, Kyoto, Japan; 20 mm × 250 mm) to provide the expected peptides. The peptides were characterized by matrix-assisted laser desorption ionization time-of-flight mass spectrometry (AXIMA-CFR plus, Shimadzu, Kyoto, Japan).

Plasmids and Arrestin BRET. The β-arrestin2-RLuc plasmid was a generous gift from M. Bouvier and has been previously described.[13] The cloning of CXCR7-YFP has been described previously.[2] All CXCR7 mutants (D179N, R197D, S198R, K206D, R197D/S198R, R197D/S198R/K206D, D275A, and D275N) were produced using polymerase chain reaction site-directed mutagenesis and verified by Sanger sequencing. Recruitment of β-arrestin2 to CXCR7 and receptor mutants was tested using a bioluminescence resonance energy transfer (BRET)-based test, as previously described.[2]

Radioligand Binding Assays. Membranes of receptor-transfected HEK293 cells were prepared as described previously.[14] Five micrograms of membrane protein was used per point. Binding was performed using 50 pM [^{125}I]CXCL12 (PerkinElmer) and indicated concentrations of the unlabeled competitor. Samples were equilibrated for 2 h at 4 °C before unbound radioactivity was separated from bound radioactivity using filtration and counting.

Molecular Modeling. Receptor residues are indexed according to the nomenclature of Ballesteros and Weinstein.[15] For homology modeling, we used the LOMETS server to generate homology structures of the CXCR7 receptor.[16] We selected a structure generated from the crystal structure of the homologue CXCR4 receptor [Protein Data Bank (PDB) entry 3odu] generated by the threading program SP3 that featured both known disulfide bonds. The model had a coverage of 0.834, a *Z* score of 30.330, a Seq_id of 0.29, and a high confidence score.[17] We slightly modified the end of ECL2 as it reached the top of TM5 to accommodate the docking of the peptide ligands in a pose similar to that of CVX15 in the crystal structure of CXCR4 (PDB entry 3OE0). The backbone of the model is very similar to the crystal structure of the CXCR4 receptor in complex with the peptide antagonist CVX15 (PDB entry 3OE0), with a root-mean-square deviation (rmsd) distance of 0.912 Å between the positions of Cα atoms. The homology model was also analyzed with ProCheck,[18] and the Ramachandran plot indicated that >99% of the residues were in the "most favored" and "additionally allowed" regions. The rest of the stereochemistry was also of high quality. The unstructured N-terminal and C-terminal portions of the model were truncated by removing residues 1−32 and 321−362, respectively, to keep the simulation box as small as possible and to permit better performances for the molecular dynamics (MD) simulations. The model of the R197D−CXCR7 receptor was generated by replacing residue R197 with an aspartate using the mutagenesis feature in PyMOL. The T140 and TZ14004 molecules were designed from the CVX15 molecule from PDB entry 3OE0 using the mutagenesis feature in PyMOL. The ligands were manually docked by superposing the T140 or TZ14004 molecule on the CXV15 molecule of the crystal structure of CXCR4 after superposing the CXCR7 receptor model on the CXCR4 receptor model.

Molecular Dynamics Simulations. The GROMACS software suite[19] was used to prepare and run the simulations. The CXCR7 and R197D−CXCR7 receptor models were inserted into a lipid bilayer consisting of 128 molecules of DOPC using the InflateGRO approach.[20] Simulation parameters were based on previous work.[21] The membrane−receptor system was solvated with the SPC water model.[22] Counterions were added at random positions, replacing water molecules, to keep the net charge of the system at 0. The ffg53a6 force field, modified to use the Berger lipids parameter,[23] was used for the calculations. Parameters for the DOPC molecules and the PDB file of the bilayer, developed by the Tieleman group,[24] were obtained from P. Tieleman's Web site (moose.bio.ucalgary.ca).The naphthalene and citrulline side chains were manually parametrized for the force field based on existing parameters of other residues. *NVT* equilibration of the system was performed for 100 ps to reach the desired temperature of 310 K. This was followed by equilibration under *NPT* conditions for 15 ns with the pressure set at 1 bar. Such a long equilibration is necessary for proper equilibration of the lipids after embedding a protein in the membrane.[25] We monitored the system's size on the *X*, *Y*, and *Z* axes to confirm the stabilization on the DOPC bilayer. The position of all heavy atoms of the receptor was restrained during equilibration. The system size after *NPT* equilibration was approximately 71 Å × 70 Å × 81 Å, ensuring that the CXCR7 receptor molecule could not interact with its periodic image. Unrestrained MD simulations were run for 4 × 20 ns in 2 fs steps, for a total of 80 ns of simulation time per receptor or receptor−ligand complex. The simulation duration of 80 ns was deemed long enough for our study, which aims to analyze side chain reorientation and, to a certain extent, movement of the ligand. These motions occur on the nanosecond time scale.[26] The simulations were run under periodic boundary conditions at constant temperature (310 K) and pressure (1 bar) using the Nose-Hoover thermostat[27,41] with a τ_T of 0.2 ps and the Parrinello−Rahman barostat with a τ_P of 5 ps, respectively. Simulation data were saved every 20 ps, for a total of 4001

DOI: 10.1021/bi501526s
Biochemistry 2015, 54, 1505−1515

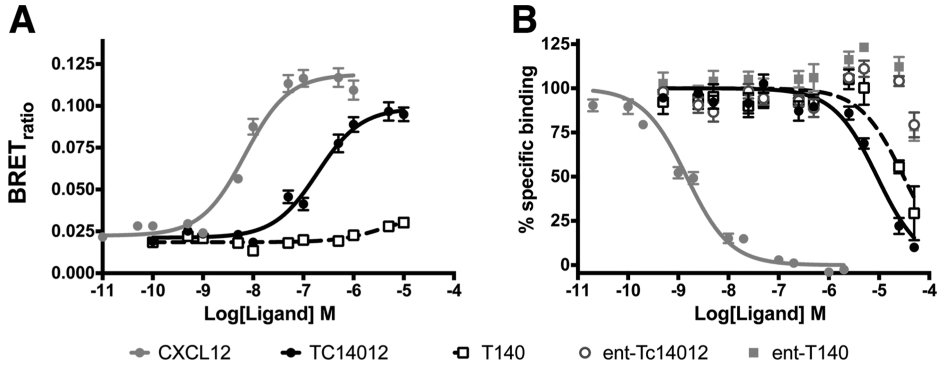

Figure 1. T140 is no CXCR7 agonist. (A) Induction of recruitment of arrestin to CXCR7 by TC14012 (black circles), T140 (empty squares), or CXCL12 (gray circles) was measured by the induction of BRET between CXCR7-YFP and β-arrestin2-RLuc. (B) Competition of TC14012 (black circles), T140 (black squares), CXCL12 (gray circles), and corresponding enantiomers [ent-TC14012 (empty circles) and ent-T140 (gray squares)] with radiolabeled CXCL12 for CXCR7 binding. The mean ± the standard error of the mean of three independent experiments, each conducted in triplicate, is shown.

Scheme 1. Sequences of the Parental T140 and the Tested Analogues[a]

Disulfide Bond

Position:	1	2	3	4	5	6	7	8	9	10	11	12	13	14
T140 :	H	Arg	Arg	Nal	Cys	Tyr	Arg	Lys	DLys	Pro	Tyr	Arg	Cit	Cys	Arg	OH
TC14003 :	H	Arg	Arg	Nal	Cys	Tyr	Cit	Lys	DLys	Pro	Tyr	Arg	Cit	Cys	Arg	OH
TC14005 :	H	Arg	Arg	Nal	Cys	Tyr	Arg	Lys	DCit	Pro	Tyr	Arg	Cit	Cys	Arg	OH
TZ14004 :	H	Arg	Arg	Nal	Cys	Tyr	Arg	Lys	DLys	Pro	Tyr	Arg	Cit	Cys	Arg	NH_2
TN14003 :	H	Arg	Arg	Nal	Cys	Tyr	Cit	Lys	DLys	Pro	Tyr	Arg	Cit	Cys	Arg	NH_2
TN14005 :	H	Arg	Arg	Nal	Cys	Tyr	Arg	Lys	DCit	Pro	Tyr	Arg	Cit	Cys	Arg	NH_2
TC14012 :	H	Arg	Arg	Nal	Cys	Tyr	Cit	Lys	DCit	Pro	Tyr	Arg	Cit	Cys	Arg	NH_2
CVX15 :	H	Arg	Arg	Nal	Cys	Tyr	Gln	Lys	Dpro	Pro	Tyr	Arg	Cit	Cys	Arg	Gly – DPro – OH

[a]The cystine bridge is conserved in all derivatives. The sequence of CVX15, which had been used for cocrystallization with CXCR4, is shown for comparison. Positions diverging between the analogues are highlighted: CVX15 (yellow), T140 (blue), and TC14012 (red).

frames. The stability of the systems was assessed by calculating the rmsd distance between the positions of Cα atoms of the TMDs during the simulations. In all instances, the rmsds converged to a similar and stable value, close to 2.5 Å, indicating that equilibrium was reached before the MD simulations were initiated. The same protocol was used for simulations of the ligands in water, except for the use of a smaller, dodecahedric box and shorter *NPT* equilibration time (200 ps) because of the absence of lipids.

Trajectory Analysis. MD trajectories output from GROMACS were converted to PDB files with 200 frames per 80 ns (1 for every 20 saved) for visual inspection with the PyMOL Molecular Graphics System (version 1.3r1) and to compressed XTC trajectory files with all frames for other analyses. Evaluation of the presence of H-bonds during the simulations was performed with the g_hbond tool in GROMACS using the default cutoff angle value of 30° and a cutoff radius of 0.35 nm. The length of the salt bridges was measured with the g_dist tool within GROMACS using the centroids of the charged groups. This corresponds to Cζ for arginine, the center of mass of the Cγ−Oδ1−Oδ2 group for aspartate, and the center of mass of the Cδ−Oε1−Oε2 group for glutamate.

RESULTS

TC14012, but Not T140, Is a CXCR7 Agonist on the Arrestin Pathway. Using the previously reported BRET-based CXCR7−β-arrestin recruitment assay, we found that the previously reported efficacious agonist activity of TC14012 on CXCR7[8] is not shared by the original compound, T140 (Figure 1A). Heterologous compound competition with [^{125}I]CXCL12 for CXCR7 binding was weak (≈10 μM), but specific, as indicated by absence of an effect of TC14012 or T140 enantiomers [ent-TC14012 and ent-T140 (Figure 1B)]. The discrepancy between TC14012 IC_{50} and arrestin recruitment EC_{50} (≈300 nM) is suggestive of allosteric interaction of the compound with the receptor. Of note, differences in IC_{50} between TC14012 and T140 were small (3−5-fold), suggesting that the absence of arrestin responses to T140 was not solely due to weak binding.

TC14012 Arg14 Amidation Is Required for CXCR7 Agonism. We then identified the determinants in TC14012 for its activity on CXCR7. As shown in Scheme 1, the differences between T140 and TC14012[11] are limited to three positions. (i) T140 Arg6 is substituted with Cit6 in TC14012, (ii) D-Lys8 substituted with D-Cit8, and (iii) the free carboxyl terminus of Arg14 amidated in TC14012. To uncover which of these differences is responsible for TC14012 agonist activity on CXCR7, we used a set of compound derivatives that differ at only some of these positions (Scheme 1). The results demonstrate that C-terminal amidation is the major determinant for agonist activity on CXCR7, as all amidated compounds (TN14005, TN14003, and TZ14004)[11] induced significant arrestin recruitment, whereas those that were not amidated

DOI: 10.1021/bi501526s
Biochemistry 2015, 54, 1505−1515

(TC14003 and TC14005)[12] did not, like T140 (Figure 2 and Table 1). In contrast, the substitutions of Arg6 and D-Lys8 with

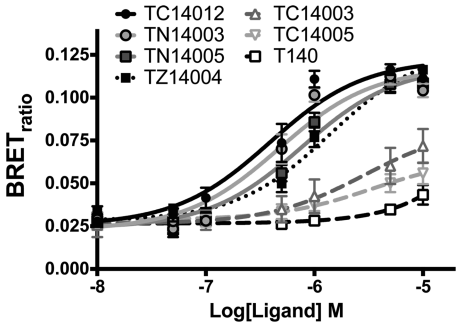

Figure 2. Recruitment of β-arrestin to CXCR7 by T140 analogues. Induction of recruitment of arrestin to CXCR7 by the analogues as tested by BRET. TC14012 (black circles) and TZ14004 (black squares), which is identical to the inactive T140 except for its amidated C-terminus, as well as TN14003 (gray circles) and TN14005 (gray squares) efficiently recruit arrestin. The Arg6 to Cit (TC14003, white pyramids) and D-Lys8 to Cit (TC14005, white triangles) substitutions have a limited effect, compared to T140 (white squares). The mean ± the standard error of the mean of three independent experiments, conducted in triplicate, is shown.

Cit6 and D-Cit8 in TC14012, respectively, contributed little to compound agonism on CXCR7. Taken together, these results suggest that Arg14 amidation in TC14012 is required for its agonist activity on CXCR7.

Arg14 Amidation Affects Compound Conformation. Previous NMR studies with T140 have shown that the compound adopts a β-hairpin structure that is stabilized by the disulfide bond between Cys4 and Cys13 and an extensive network of intramolecular backbone interactions.[28] In CXCR4, T140 Arg14 is part of a bipartite pharmacophore that consists of Arg14 (with Arg1, Nal3, and Tyr5) on one hand and Arg2 on the other.[12] Importantly, the hairpin fold extends beyond the disulfide bond and involves the Arg2 and Arg14 pharmacophores. We thus considered that these intramolecular interactions could be altered by Arg14 amidation and thereby change the overall conformation and the orientation of the pharmacophores.

To test this hypothesis, we performed molecular dynamics simulations of the T140 and TZ14004 [T140 with Arg14 amidation (Scheme 1)] ligands in water to evaluate the impact of the C-terminal amidation on their structure. The results of these simulations are shown in Figure 3. We found overall compound conformation is indeed affected, and this effect concerns particularly residues Arg1 and Arg2, which show significantly increased conformational flexibility in TZ14004 (Figure 3A). This results from the H-bonds formed by the C-terminal moiety, as the T140 carboxylate can form simultaneous H-bonds with the backbone amides of both Arg2 and Nal3, thus restraining torsion of the ψ angle of Arg2 within close limits (Figure 3B). In contrast, the amidated C-terminal moiety of TZ14004 forms only one H-bond with the backbone amide of Nal3. Accordingly, the mean distance between the Cα atoms of Arg2 and Arg14 of TZ14004 is increased, with greater liberty of movement (from 5.6 ± 0.3 Å in T140 to 6.1 ± 1.1 Å for TZ14004). This increased conformational flexibility of the pharmacophores provided by Arg14 amidation in TC14012 and TZ14004 could facilitate the formation of critical salt bridges of Arg2 and Arg14 with their respective interaction partners.

The Interaction of the Compound with CXCR7 Is Similar to That with CXCR4. To identify TC14012 Arg2 and Arg14 interaction determinants in CXCR7, we resorted to receptor mutagenesis (for an overview of the mutants tested in this study, see Scheme 2A). In the crystal structure of CXCR4 in complex with the T140 derivative antagonist CVX15 (see Scheme 1), Arg14 forms an ionic interaction with residue D262 of CXCR4 ($D^{6.58}$ following the nomenclature of Ballesteros and Weinstein[15]), at the junction of TM6 and ECL3.[10] Arg2, in turn, interacts with CXCR4 D171 ($D^{4.60}$) at the junction of TM4 and ECL2, and with parts of the second extracellular loop, ECL2 (see below). In CXCR7, residues $D^{4.60}$ and $D^{6.58}$ are conserved as $D179^{4.60}$ and $D275^{6.58}$, respectively. To test whether they are also essential for TC14012 agonism on CXCR7, and thus whether the mode of binding to both receptors is similar, we mutated CXCR7 $D^{4.60}$ to D179N and $D^{6.58}$ to D275N and D275A. Like all receptor mutants used in this study, the mutants were expressed at the cell surface to degrees similar to that of wild-type CXCR7 (Figure S1 of the Supporting Information).

As shown in Figure 4A, mutant D179N responded well to CXCL12, but there was no response to either TC14012 or T140. Similar observations were made with mutants D275N and D275A, as both mutations abolished TC14012 responses (Figure 4B,C), while CXCL12 responses were conserved [though altered (Figure 4D)]. These results show that CXCR7 $D179^{4.60}$ and $D275^{6.58}$ are indeed required for TC14012 agonism, in line with similar modes of binding of T140-derived compounds to CXCR4 and CXCR7. Taken together, these results reveal similarities of the mode of binding of the compound to CXCR4 and CXCR7 by engaging $D^{4.60}$ and $D^{6.58}$, probably with the same compound pharmacophore residues Arg14 (engaging $D^{6.58}$) and Arg2 (engaging $D^{4.60}$), respectively.

Mutation of CXCR7 ECL2 Allows T140 Agonist Activity. Important CVX15−CXCR4 interaction determinants are located in the second extracellular loop (ECL2).[10] CXCR7 ECL shows very little homology with CXCR4 ECL2 (Scheme 2B). Key residues D187 and R188 of CXCR4 adjacent to the conserved cysteine that links ECL2 to the top of TM3 (and that interact with CVX15 positions 1−4) and D193 (interacting with Lys7) are not conserved in CXCR7 (which has R197, S198, and K206 instead). To assess the role of this domain in CXCR7, we constructed and tested the triple mutant R197D/S198R/K206D [DRD mutant (Scheme 2A)], in which key CXCR4 ECL2 residues are introduced into CXCR7 ECL2. As shown in Figure 5A, this triple mutant responds weakly to CXCL12. However, surprisingly, T140 now efficiently activated arrestin recruitment, while the response to TC14012 [and

Table 1. EC_{50} Values of the TC14012 Derivatives

	TC14012	TN14003	TN14005	TZ14004	TC14003	TC14005	T140
log EC_{50}	−6.41 ± 0.09	−6.33 ± 0.08	−6.11 ± 0.08	−5.85 ± 0.09	−5.54 ± 0.39	5.467 ± 0.39	N/A
EC_{50} (nM)	388	469	769	1409	2860	3411	N/A

DOI: 10.1021/bi501526s
Biochemistry 2015, 54, 1505−1515

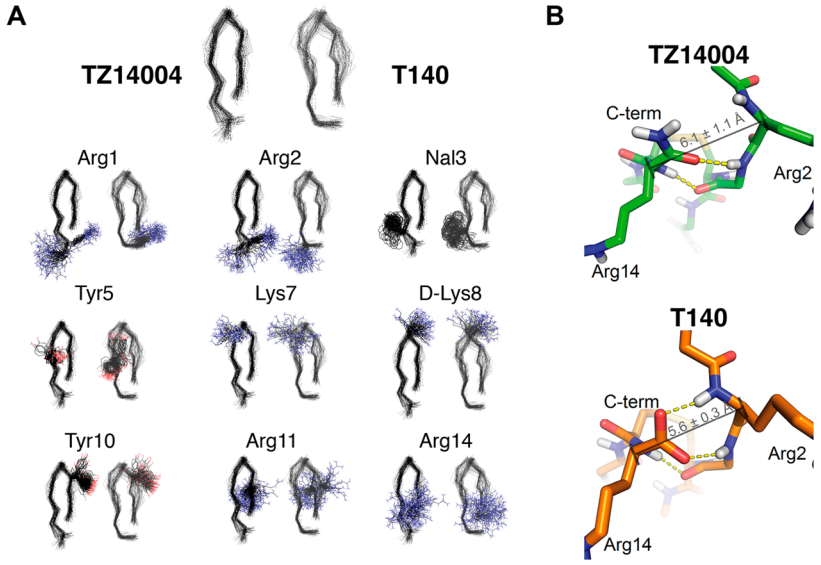

Figure 3. Conformations of TZ14004 and T140 in solution during MD simulations. (A) Comparison of the orientation of individual side chains for TZ14004 (black) on the left and T140 (dark gray) on the right. Four hundred structures covering 80 ns of MD simulations are superimposed. (B) Representative snapshots of the MD simulations showing the H-bonds (yellow dashes) formed between the C-terminal moiety of TZ14004 (green) or T140 (orange) and backbone amides. The average distance and standard deviation between the Cα atoms of residues Arg14 and Arg2 during the MD simulations are shown. Backbones of ligands are shown as a thin trace and side chains as lines. Oxygen atoms are colored red, nitrogen atoms blue, hydrogen atoms white, and carbon atoms as indicated.

Scheme 2. (A) CXCR7 Snakeplot with Residues Mutated in This Study Highlighted in Black and (B) Sequence Alignment of CXCR7 and CXCR4 Extracellular Loop 2 (ECL2)[a]

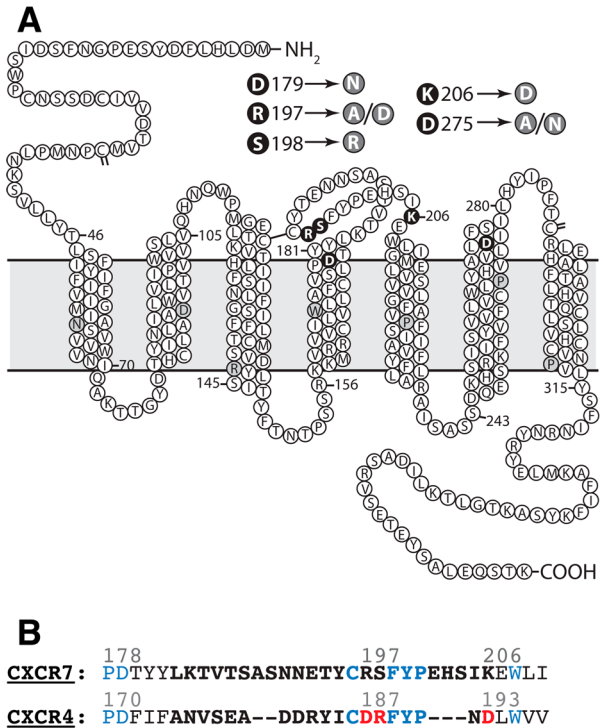

[a]ECL2 residues are represented in bold, the conserved residues in blue, and the amino acids of CXCR4 that were shown to interact with CVX15 in the crystal structure in red.

TZ14004 (not shown)] was somewhat compromised. Similar results were obtained with the R197D/S198R double substitution that still affected the response to TC14012 (Figure 5B), while the responses of single mutant K206D (corresponding to CXCR4 D193, which engages CVX15 Lys7) were unaltered compared to those of wild-type CXCR7 (Figure 5C). R197 and S198 lie just behind the conserved cysteine residue in ECL2 and correspond to positions ECL2b C + 1 and ECL2b C + 2,[29] respectively, and are thus tethered to the top of TM3. Testing CXCR7 single mutants R197D and S198R to further break down their respective contributions revealed that the S198R substitution alone was sufficient to completely abolish either T140 or TC14012 activity (Figure 5D), while both compounds were agonists with very similar potency and efficacy on CXCR7 R197D (Figure 5E). The nonresponsiveness of S198R is potentially due to the creation of strong repulsive forces between the two adjacent arginines, R197 and R198, in this mutant and Arg1 and Arg2 in the compounds. To test this, we constructed mutant R197A, which has no basic residues, but does not mimic CXCR4 D193. This mutation dramatically increased the potency of TC14012 from an EC_{50} of 390 nM on wild-type (WT) CXCR7 to 14 nM on the R197A mutant, equal to the potency of the endogenous agonist CXCL12 (Figure 5F). This indicates that, indeed, CXCR7 R197 contributes to the low potency of TC14012 on CXCR7, presumably via repulsive forces with the positively charged compound. T140 was only weakly efficient on R197A, however, although the response potency was essentially unaltered compared to that of R197D. This suggests that the introduction of D197, and not just the removal of the repulsive R197, allowed T140 to efficiently promote arrestin recruitment. Interestingly, the increased efficacy of T140 on R197D when compared to that of R197A was not reflected by the improved displacement of [^{125}I]CXCL12, which remained in the IC_{50} micromolar range (Figure 5G,H). Similarly, the increased potency of TC14012 on R197A was accompanied by an only very moderate increase in IC_{50}, which remained far from the EC_{50} [IC_{50} of >700 nM and arrestin recruitment EC_{50} of 14 nM (compare panels F and H of Figure 5)], again in line with an allosteric binding mode.

DOI: 10.1021/bi501526s
Biochemistry 2015, 54, 1505−1515

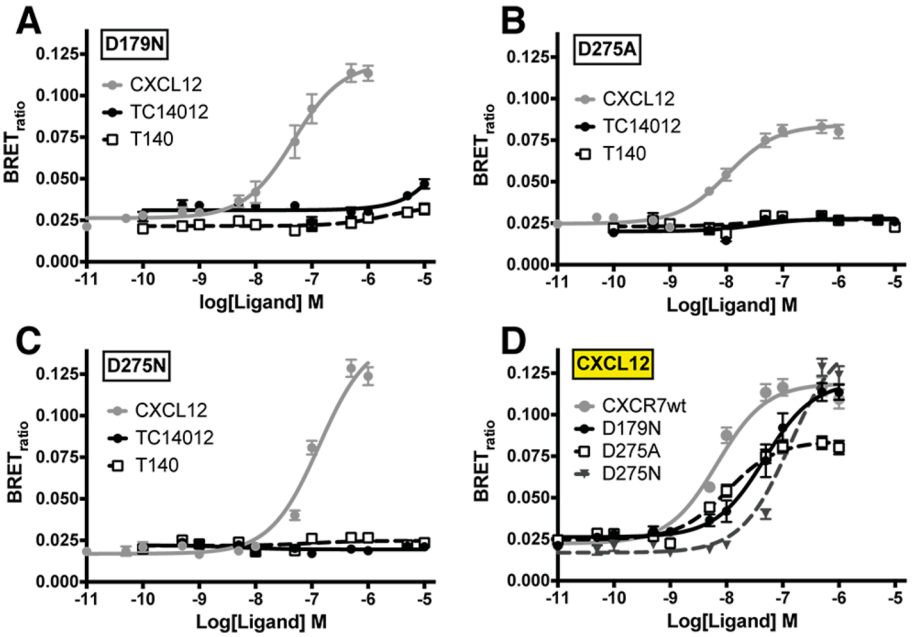

Figure 4. Recruitment of β-arrestin to CXCR7 D179A and D275 mutants. (A–C) Induction of recruitment of arrestin to CXCR7 mutants by T140 (white squares) and TC14012 (black circles), using CXCL12 (gray circles) as a control. (D) Differences in CXCL12 activity on mutants D179N (black circles), D275A (black squares), and D275N (gray triangles) compared to that of wild-type CXCR7 (gray circles). While D275N and D179N affect the potency of the response, D275A affects the efficacy. The mean ± the standard error of the mean of three independent experiments, conducted in triplicate, is shown.

MD Simulations Reveal a Weakened Ability of T140 To Form Simultaneously Critical Salt Bridges in WT CXCR7. To further rationalize the structural basis of the findings described above, we performed molecular dynamics simulations with T140 or TZ14004 docked in complex with either CXCR7 or R197D CXCR7. Each receptor–ligand complex was simulated in quadruplicate for 20 ns, for a total of 80 ns of MD simulation time for each complex. TZ14004, rather than TC14012, was chosen for modeling to specifically address the role of the C-terminal amidation.

The MD simulations indicated that the CXCR7–ligand complexes are dynamic entities with much movement from the side chains. Nonetheless, three sectors in the WT CXCR7 receptor were identified that accommodate the side chains of residues Arg1, Arg2, and Arg14 of both ligands (Figure 6A). Arg1 and the N-terminal moiety formed H-bonds with H298 and Q301 (in TM7). Arg2 formed a salt bridge and, when distance and orientation permitted it, H-bonds with D179 (TM4). It could also form H-bonds with the surrounding side chains of Y200 (ECL2), S216 (TM5), and Y268 (TM6) as it was reoriented. Similarly, Arg14 formed a salt bridge (and H-bonds when permitted) with D275 (TM6), but as it was reoriented, it could also interact with the nearby S278 (H-bond) and E290 (salt bridge and H-bonds), at the junctions of ECL3 with both TM6 and TM7, respectively. In addition, a dynamic H-bond network was observed between CXCR7 ECL2 and residues of the compound hairpin (positions 3–12), with no striking difference between T140 and TC14012 (not shown). The main difference in MD simulations with the R197D CXCR7 mutant was that the N-terminal moiety and the Arg1 side chain were now reoriented in both T140 and TZ14004 to form a salt bridge with residue R197D, similar to the salt bridge formed between Arg1 and CXCR4 D187 in the CVX15–CXCR4 crystal (Figure 6B).[10]

In terms of observed interactions, no obvious singular differences between T140 and TC14012 could explain the inability of T140 to activate CXCR7. We thus explored the possibility that the more relaxed conformation of the TZ14004 pharmacophore (Figure 3B) facilitates the simultaneous formation of the critical salt bridges (between Arg2 and D179 and between Arg14 and D275). We further hypothesized that the R197D mutation might favor such simultaneous salt bridges by moving Arg2 closer to D179 as a consequence of the repositioning of Arg1 in the R197D mutant.

To verify this claim, we monitored the distance between the charged groups of the two critical salt bridges during the MD simulations. The resulting graphs indicated that, for the T140–WT CXCR7 complex, the two salt bridges were indeed rarely simultaneously <5 Å in length (Figure S2A of the Supporting Information), a distance proposed as a cutoff beyond which salt bridges become destabilized, the enthalpic gain being too small to compensate for the entropic loss.[30] In addition, they appeared to be alternating in length, with either Arg2 being close to D179 or Arg14 being close to D275. This contrasted with the other three complexes (T140–R197D CXCR7, TZ14004–WT CXCR7, and TZ14004–R197D CXCR7), where indeed simultaneous salt bridges <4–5 Å in length were observed (Figure S2B–D of the Supporting Information). To further substantiate these observations and to evaluate the best binding conformation that can be attained, we analyzed the trajectories of each ligand–receptor complex individually for both salt bridge simultaneity and length (Table S1 of the Supporting Information). In the best of the four trajectories, simultaneous salt bridges <5 Å in length were present only one-fourth (25.6%) of the time for the T140–WT CXCR7 complex, compared to two-thirds (66.4%) of the time for the TZ14004–WT CXCR7 complex. In addition, the strongest, shortest salt bridges for the T140–WT CXCR7 complex had a sum length of 10.68 ± 1.74 Å, which was decreased to 8.84 ±

DOI: 10.1021/bi501526s
Biochemistry 2015, 54, 1505–1515

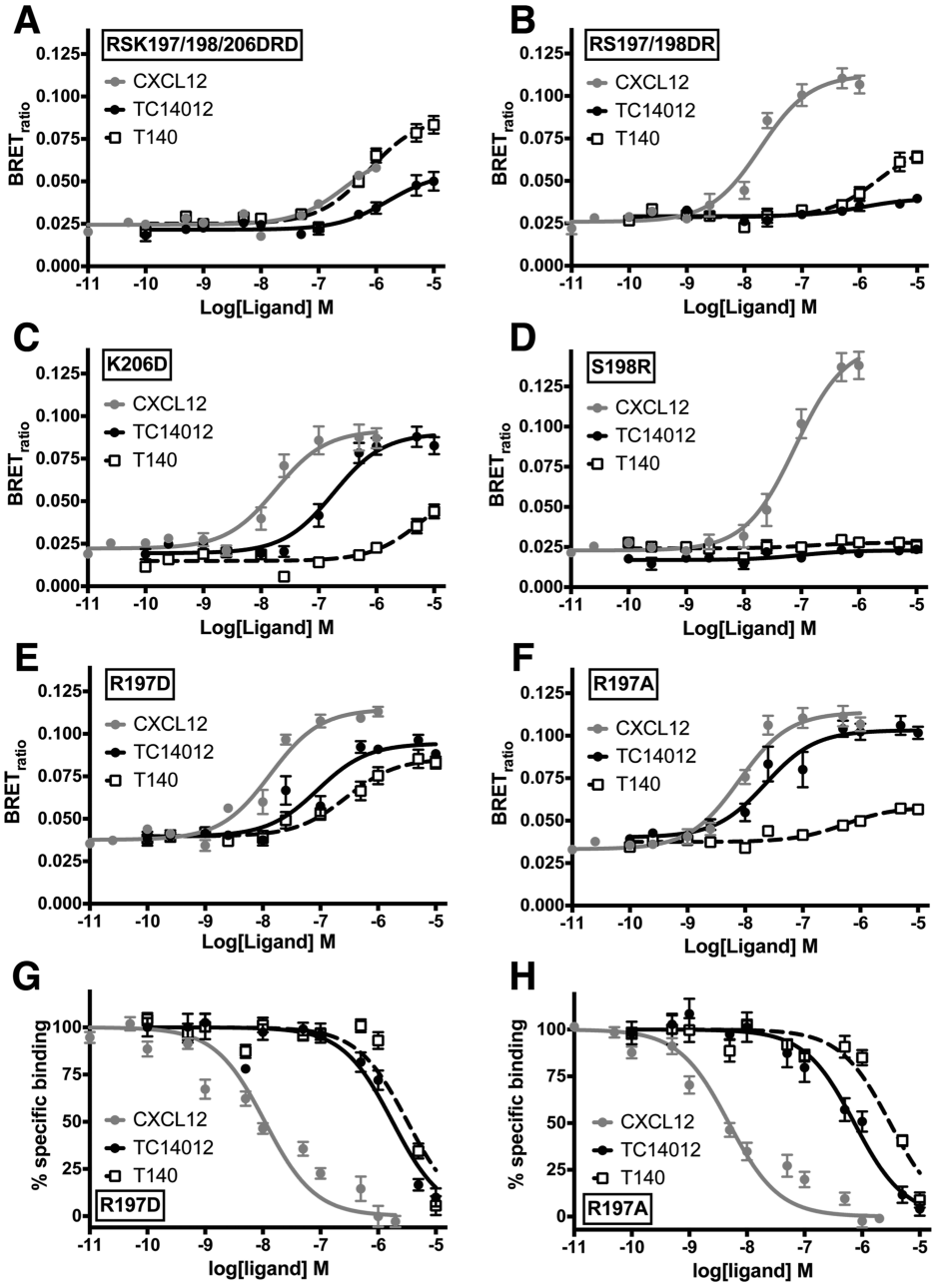

Figure 5. Recruitment of β-arrestin to CXCR7 ECL2 mutants. (A–F) Induction of recruitment of arrestin to CXCR7 mutants by T140 (white squares) and TC14012 (black circles), using CXCL12 (gray circles) as a control. Note the efficient response to T140 in panels A, B, and E. (G and H) Binding competition of CXCL12, TC14012, and T140 with radiolabeled CXCL12 for CXCR7 binding. The mean ± the standard error of the mean of at least three independent experiments, conducted in triplicate, is shown.

1.46 Å for the TZ14004–WT CXCR7 complex. Accordingly, the Arg2–D179 salt bridge of the T140–WT CXCR7 complex has an average length of 6.19 ± 1.50 Å, which is more than 2 Å longer than in the TZ14004–WT CXCR7 trajectory. These shortcomings of the T140–CXCR7 complex were indeed not observed in the T140–R197D CXCR7 complex. Here, simultaneous salt bridges <5 Å in length with D179 and D275 occurred at an increased rate of 41.3% of the time; the sum of the length of both bonds decreased to 9.50 ± 0.87 Å, and the Arg2–D179 distance was indeed decreased to 4.21 ± 0.48 Å (more than 2 Å).

We also monitored other possible salt bridges formed by Arg2 and Arg14, with residues E213$^{5.39}$ (top of TM5) and E290$^{7.28}$ (ECL3 and TM7). The salt bridge between Arg14 and E290$^{7.28}$ was the only one to be consistently formed at a somewhat short distance in the trajectories where aforementioned critical salt bridges were at their shortest, averaging 7.36 ± 1.33 Å for the T140–R197D CXCR7 complex, 6.01 ± 0.92 Å for the TZ14004–WT CXCR7 complex, and 5.96 ± 0.89 Å for the TZ14004–R197D CXCR7 complex (Figure S2A–D of the Supporting Information). This pattern was, however, not observed for the T140–WT CXCR7 complex as this salt bridge was 12.38 ± 2.36 Å in length in the corresponding trajectory, which is beyond the generally accepted cutoff length of 8–10 Å for salt bridges in water because of the dielectric constant of water rendering the interaction negligible.[31]

Overall, the analysis of the MD simulations indicates that T140 forms weaker critical salt bridges over longer distances in

DOI: 10.1021/bi501526s
Biochemistry 2015, 54, 1505–1515

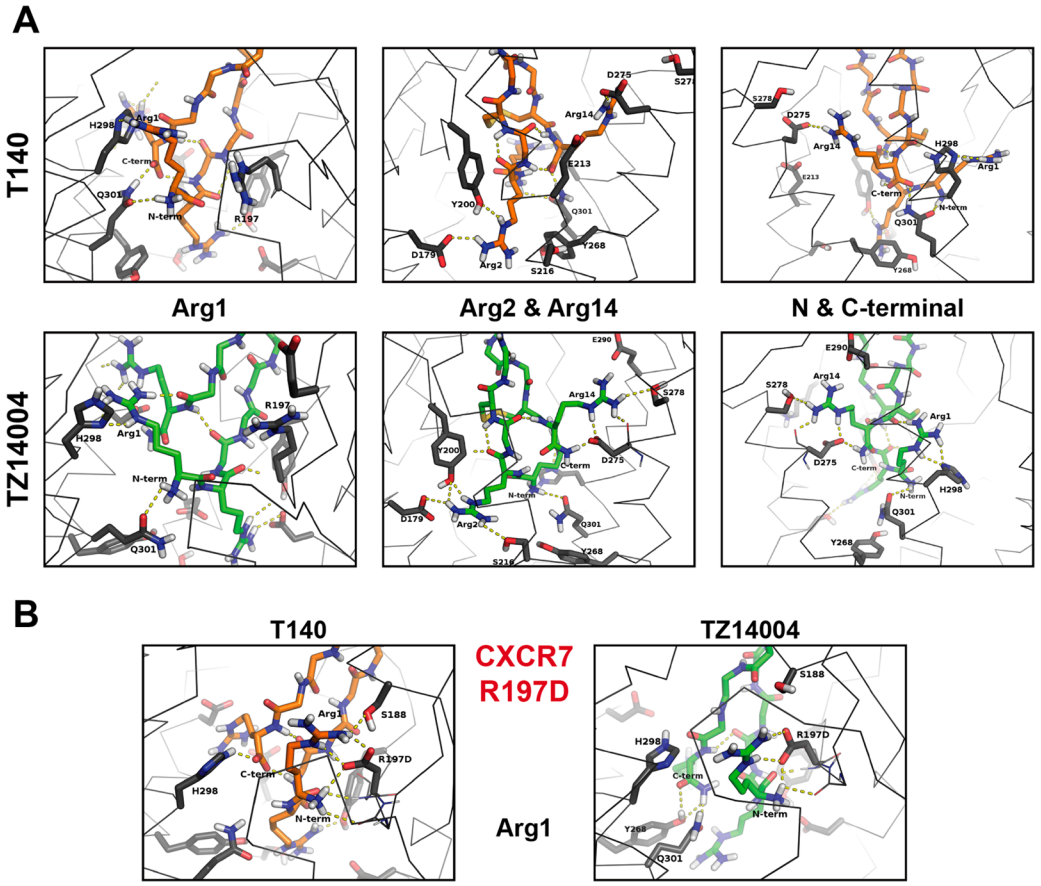

Figure 6. H-Bonds formed between ligands and CXCR7. Representative snapshots from MD simulations showing the polar environments and potential H-bond partners of the receptor (gray) stabilizing charged side chains of T140 (orange) and TZ14004 (green). (A) Arg1 and the N-terminal moiety can form H-bonds with H298 and Q301 (in TM7). Arg2 can form H-bonds with D179 (TM4), Y200 (ECL2), S216 (TM5), and Y268 (TM6). Arg14 can form H-bonds with D275 (TM6), S278 (TM6), and E290 (TM7). (B) In the R197D CXCR7 mutant receptor, the N-terminal Arg1 side chain can form H-bonds with D197.

the wild-type CXCR7 receptor, which as a consequence thwarts simultaneous engagement of the clamp positons in TM4 and TM6. The longer distance between Arg14 and E290$^{7.28}$ with T140 in the wild-type CXCR7 receptor is also indicative of a slightly different binding conformation for this complex. However, T140 Arg1 interacts with mutant receptor D197, which reorients Arg2 closer to D179 in TM4 and facilitates simultaneous recognition of D179 and D275, thereby permitting receptor activation.

DISCUSSION

This work reports the mode of binding of TC14012 to CXCR7, combining receptor mutagenesis and the use of compound derivatives with molecular modeling to further rationalize the experimental findings. Given that TC14012 is a known antagonist of the canonical chemokine receptor CXCR4, which shares the chemokine ligand CXCL12 with CXCR7, but, in contrast, activates the arrestin pathway on CXCR7, our study yields insight into the unusual activation mechanism of CXCR7.

Mode of TC14012−CXCR7 Binding. Overall, we find striking similarities between the mode of binding of TC14012 to CXCR7 and the mode of binding of its derivative CVX15 to CXCR4.[10] In both circumstances, receptor residues D$^{4.60}$ and D$^{6.58}$ play key roles to form salt bridges with the compound pharmacophore Arg2 and Arg14, respectively. In addition, H-bond interactions with CXCR7 ECL2 (but no salt bridges as in CXCR4) are observed, so that, like in CXCR4, TC14012 roughly covers the major binding pocket formed by TM3−TM7 (Scheme 3). Of note, the identified key residues are similar to those reported for other CXCR4 antagonists. CXCR4 D171$^{4.60}$ and D187 (ECL2b Cys + 1) are key residues for cyclic pentapeptide FC131.[32] In addition, the Food and Drug

Scheme 3. CXCR7 Helical Wheel Diagram Seen from the Extracellular Side of the Receptor, with Parts of ECL2[a]

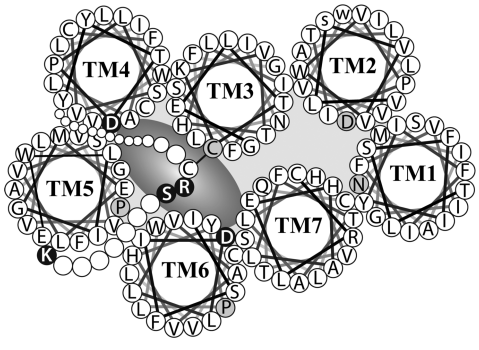

[a]Residues highlighted in black were mutated in this study. The grey oval indicates TC14012 positioned in the major binding pocket between TM3 and TM7.

DOI: 10.1021/bi501526s
Biochemistry 2015, 54, 1505−1515

Administration-approved CXCR4 antagonist AMD3100 also depends on $D^{4.60}$ and $D^{6.58}$, with some contribution from ECL2.[33,34] Therefore, the agonistic (on CXCR7) TC14012 adopts a mode of binding to CXCR7 that resembles that of binding of antagonists to CXCR4. A recent virtual screening approach suggests that this feature may be shared by other small CXCR7 ligands. Yoshikawa et al. developed a CXCR7 model that highlights CXCR7 positions $D179^{4.60}$ and $D275^{6.58}$ as key residues of the receptor pharmacophore.[35] Indeed, $D^{4.60}$ and $D^{6.58}$ were engaged by all four reference CXCR7 ligands, two of which were derived from the patent literature. Although arrestin recruitment experiments were not described, it is tempting to speculate that these small ligands also activate CXCR7 given that all reported compounds of the Chemocentryx CCX series are CXCR7 agonists.[7,36] Of note, another series of compounds, similar to the CCX compounds based on styrene-amides, all turned out to be CXCR7 agonists.[9]

T140. In contrast to TC14012, its parent compound, T140, was almost devoid of CXCR7 agonist activity, despite binding competition with CXCL12 that was only slightly inferior to that with TC14012 and no obvious differences in CXCR7 engagement when modeled. This resulted from the lack of flexibility in the T140 pharmacophore due to intramolecular interaction with the free T140 carboxyl terminus[28] that resulted in a constrained compound conformation. This constraint was released in the C-terminally amidated TC14012, resulting in much greater pharmacophore flexibility. The constrained T140 conformation favored only alternate but not simultaneous engagement of CXCR7 $D179^{4.60}$ by Arg2 and $D275^{6.58}$ by Arg14. This shortcoming was adjusted by the introduction of the R197D mutation, which led to interaction of T140 Arg1 with D197, analogous to what was observed in the CVX15−CXCR4 crystal.[10] This new interaction realigned T140 Arg2 with $D179^{4.60}$, thereby stabilizing the compound in an orientation that permitted simultaneous Arg14−$D275^{6.58}$ engagement. These data point toward a necessity for CXCR7 agonists to concurrently interact with the upper parts of TM4 and TM6 to draw them together or, alternatively, push them apart, possibly involving TM3.

Role of ECL2. The role played by CXCR7 ECL2 was difficult to assess. Indeed, CXCR7 ECL2 is very different from CXCR4 ECL2 in both amino acid sequence and length, resulting in potential shortcomings in the molecular model we used. Nevertheless, H-bond networks resembling those seen between CVX15 and CXCR4 were observed. It became clear that residues ECL2b Cys + 1 and Cys + 2 (R197 and S198, respectively) are important. While substitution of R197D stabilized the orientation of T140 by creating a salt bridge with Arg1, removal of the charge with the R197A substitution failed to do so but nevertheless resulted in a much higher potency of activation by TC14012, which equaled that of CXCL12 on that mutant (14 nM). This suggests that the repulsive force of CXCR7 R197 is the major reason for the relatively weak potency of the compound on CXCR7. Why a similar effect was not observed with R197D remains unclear but may be related to the overall conformation of this part of ECL2. Similarly, the S198R single substitution was prohibitive for activity, probably by repulsion of the positively charged compound by R197 and R198. A similarly repulsive effect of CXCR4 R188 was already proposed to impinge on FC131 potency.[32]

Mode of CXCR7−Arrestin Activation. In CXCR4, FC131, T140, and AMD3100 are believed to exert their antagonistic effect by denying access of the N-terminus of CXCL12 to the interaction with an elusive "site II", thought to lie deeper in the binding crevice.[10,37] One conclusion that can thus be drawn from our results is that CXCR7 apparently does not require this second step to recruit arrestin. Rather, ligand−receptor interactions close to the receptor surface seem to be sufficient to trigger CXCR7 activation, without the need for interactions deep into the binding pocket. Indeed, comparison of the ligand binding pockets between different GPCRs revealed an outstandingly shallow interaction of CVX15 with CXCR4.[38] While this may be unsurprising for a receptor antagonist, it is rather unexpected for a receptor agonist. Along these lines of interpretation, we have previously reported AMD3100 to induce recruitment of arrestin to CXCR7.[2] Given that AMD3100 relies, like TC14012, on CXCR4 $D171^{4.60}$ and $D262^{6.58}$, we may speculate that AMD3100 also adopts a similar binding mode with CXCR7, using $D179^{4.60}$ and $D275^{6.58}$. This concurrence points toward a common, unusual mechanism by which the compounds trigger CXCR7 activation.

One of the hallmarks of agonists, as opposed to antagonists, is that they induce receptor movements that lead to signal transmission. The nature of such movements is difficult to derive from ligand fitting in static receptor models. It is, however, tempting to speculate that, for the recruitment of arrestin to CXCR7 to occur, and unlike in CXCR4 where TC14012 does not induce arrestin recruitment,[8] TM rearrangement via the interaction with their tops can already lead to TM tilting or rotational movements that trigger signal transmission.

If, and how, these findings relate to the CXCR7 activation mechanism by its endogenous chemokine ligands CXCL12 and CXCL11 remains to be seen. The inability of CXCR7 to signal via G-protein-mediated pathways is still unexplained, but CXCR7 coupling, though not activation, with $G\alpha_i$ has been described in reconstituted systems.[39] Moreover, a few cell types seem to be permissive for CXCR7-mediated G-protein activation.[40] It is tempting to speculate that CXCR7 engagement by chemokines rapidly activates G-protein-independent arrestin recruitment by superficial receptor engagement. This in turn could precede and thus prevent G-protein activation, which would necessitate "site II" engagement. Further work will be required to test these hypotheses.

In summary, we have established that CXCR4 antagonists that also bind CXCR7 do so by very similar binding modes. Their opposite effects on both receptors are thus not explained by distinct receptor engagement. Rather, CXCR7 activation of the arrestin pathway is readily triggered by interactions with the receptor surface, bypassing the need for site II interactions deep in the receptor ligand binding pocket.

■ ASSOCIATED CONTENT

Supporting Information

CXCR7 and mutant surface expression (Figure S1), simulation trajectories (Figure S2), and simulation trajectory results (Table S1). This material is available free of charge via the Internet at http://pubs.acs.org.

■ AUTHOR INFORMATION

Corresponding Author

*E-mail: nikolaus.heveker@recherche-ste-justine.qc.ca.

Author Contributions

N.M. and J.C. contributed equally to this work.

DOI: 10.1021/bi501526s
Biochemistry 2015, 54, 1505−1515

Funding

This work was supported by the Canadian Institutes for Health Research (Grant MOP123421) and by Grants-in-Aid for Scientific Research and a Core-to-Core Program from the Japan Society for the Promotion of Science (JSPS) and the Platform for Drug Discovery, Informatics, and Structural Life Science from the Japanese Ministry of Education, Culture, Sports, Science, and Technology (MEXT).

Notes

The authors declare no competing financial interest.

■ ABBREVIATIONS

CXCR4, CXC chemokine receptor 4; CXCR7, CXC chemokine receptor 7; CXCL12, CXC chemokine ligand 12; BRET, bioluminescence resonance energy transfer; TM, transmembrane domain; ECL, extracellular loop; R-Luc, *Renilla* luciferase; YFP, yellow fluorescent protein.

■ REFERENCES

(1) Burns, J. M., Summers, B. C., Wang, Y., Melikian, A., Berahovich, R., Miao, Z., Penfold, M. E., Sunshine, M. J., Littman, D. R., Kuo, C. J., Wei, K., McMaster, B. E., Wright, K., Howard, M. C., and Schall, T. J. (2006) A novel chemokine receptor for SDF-1 and I-TAC involved in cell survival, cell adhesion, and tumor development. *J. Exp. Med. 203* (9), 2201−2213.

(2) Kalatskaya, I., Berchiche, Y. A., Gravel, S., Limberg, B. J., Rosenbaum, J. S., and Heveker, N. (2009) AMD3100 is a CXCR7 ligand with allosteric agonist properties. *Mol. Pharmacol. 75* (5), 1240−1247.

(3) Rajagopal, S., Kim, J., Ahn, S., Craig, S., Lam, C. M., Gerard, N. P., Gerard, C., and Lefkowitz, R. J. (2010) β-Arrestin- but not G protein-mediated signaling by the "decoy" receptor CXCR7. *Proc. Natl. Acad. Sci. U.S.A. 107* (2), 628−632.

(4) Miao, Z., Luker, K. E., Summers, B. C., Berahovich, R., Bhojani, M. S., Rehemtulla, A., Kleer, C. G., Essner, J. J., Nasevicius, A., Luker, G. D., Howard, M. C., and Schall, T. J. (2007) CXCR7 (RDC1) promotes breast and lung tumor growth in vivo and is expressed on tumor-associated vasculature. *Proc. Natl. Acad. Sci. U.S.A. 104* (40), 15735−15740.

(5) Wang, J., Shiozawa, Y., Wang, J., Wang, Y., Jung, Y., Pienta, K. J., Mehra, R., Loberg, R., and Taichman, R. S. (2008) The role of CXCR7/RDC1 as a chemokine receptor for CXCL12/SDF-1 in prostate cancer. *J. Biol. Chem. 283* (7), 4283−4294.

(6) Hattermann, K., Held-Feindt, J., Lucius, R., Muerkoster, S. S., Penfold, M. E., Schall, T. J., and Mentlein, R. (2010) The chemokine receptor CXCR7 is highly expressed in human glioma cells and mediates antiapoptotic effects. *Cancer Res. 70* (8), 3299−3308.

(7) Zabel, B. A., Wang, Y., Lewen, S., Berahovich, R. D., Penfold, M. E., Zhang, P., Powers, J., Summers, B. C., Miao, Z., Zhao, B., Jalili, A., Janowska-Wieczorek, A., Jaen, J. C., and Schall, T. J. (2009) Elucidation of CXCR7-mediated signaling events and inhibition of CXCR4-mediated tumor cell transendothelial migration by CXCR7 ligands. *J. Immunol. 183* (5), 3204−3211.

(8) Gravel, S., Malouf, C., Boulais, P. E., Berchiche, Y. A., Oishi, S., Fujii, N., Leduc, R., Sinnett, D., and Heveker, N. (2010) The peptidomimetic CXCR4 antagonist TC14012 recruits β-arrestin to CXCR7: Roles of receptor domains. *J. Biol. Chem. 285* (49), 37939−37943.

(9) Wijtmans, M., Maussang, D., Sirci, F., Scholten, D. J., Canals, M., Mujic-Delic, A., Chong, M., Chatalic, K. L., Custers, H., Janssen, E., de Graaf, C., Smit, M. J., de Esch, I. J., and Leurs, R. (2012) Synthesis, modeling and functional activity of substituted styrene-amides as small-molecule CXCR7 agonists. *Eur. J. Med. Chem. 51*, 184−192.

(10) Wu, B., Chien, E. Y., Mol, C. D., Fenalti, G., Liu, W., Katritch, V., Abagyan, R., Brooun, A., Wells, P., Bi, F. C., Hamel, D. J., Kuhn, P., Handel, T. M., Cherezov, V., and Stevens, R. C. (2010) Structures of the CXCR4 chemokine GPCR with small-molecule and cyclic peptide antagonists. *Science 330* (6007), 1066−1071.

(11) Tamamura, H., Omagari, A., Hiramatsu, K., Gotoh, K., Kanamoto, T., Xu, Y., Kodama, E., Matsuoka, M., Hattori, T., Yamamoto, N., Nakashima, H., Otaka, A., and Fujii, N. (2001) Development of specific CXCR4 inhibitors possessing high selectivity indexes as well as complete stability in serum based on an anti-HIV peptide T140. *Bioorg. Med. Chem. Lett. 11* (14), 1897−1902.

(12) Tamamura, H., Omagari, A., Oishi, S., Kanamoto, T., Yamamoto, N., Peiper, S. C., Nakashima, H., Otaka, A., and Fujii, N. (2000) Pharmacophore identification of a specific CXCR4 inhibitor, T140, leads to development of effective anti-HIV agents with very high selectivity indexes. *Bioorg. Med. Chem. Lett. 10* (23), 2633−2637.

(13) Perroy, J., Adam, L., Qanbar, R., Chenier, S., and Bouvier, M. (2003) Phosphorylation-independent desensitization of GABA(B) receptor by GRK4. *EMBO J. 22* (15), 3816−3824.

(14) Kaya, A. I., Onaran, H. O., Ozcan, G., Ambrosio, C., Costa, T., Balli, S., and Ugur, O. (2012) Cell contact-dependent functional selectivity of β2-adrenergic receptor ligands in stimulating cAMP accumulation and extracellular signal-regulated kinase phosphorylation. *J. Biol. Chem. 287* (9), 6362−6374.

(15) Ballesteros, J., and Weinstein, H. (1995) Integrated Methods for the Construction of Three-Dimensional Models and Computational Probing of Structure-Function Relations in G-Protein-Coupled Receptors. *Methods Neurosci. 25*, 366−428.

(16) Wu, S., and Zhang, Y. (2007) LOMETS: A local meta-threading-server for protein structure prediction. *Nucleic Acids Res. 35* (10), 3375−3382.

(17) Zhou, H., and Zhou, Y. (2005) Fold recognition by combining sequence profiles derived from evolution and from depth-dependent structural alignment of fragments. *Proteins 58* (2), 321−328.

(18) Laskowski, R. A., Rullmannn, J. A., MacArthur, M. W., Kaptein, R., and Thornton, J. M. (1996) AQUA and PROCHECK-NMR: Programs for checking the quality of protein structures solved by NMR. *J. Biomol. NMR 8* (4), 477−486.

(19) Van Der Spoel, D., Lindahl, E., Hess, B., Groenhof, G., Mark, A. E., and Berendsen, H. J. (2005) GROMACS: Fast, flexible, and free. *J. Comput. Chem. 26* (16), 1701−1718.

(20) Kandt, C., Ash, W. L., and Tieleman, D. P. (2007) Setting up and running molecular dynamics simulations of membrane proteins. *Methods 41* (4), 475−488.

(21) Lemkul, J. A., and Bevan, D. R. (2009) Perturbation of membranes by the amyloid β-peptide: A molecular dynamics study. *FEBS J. 276* (11), 3060−3075.

(22) Berweger, C. D., Vangunsteren, W. F., and Mullerplathe, F. (1995) Force-Field Parametrization by Weak-Coupling: Reengineering Spc Water. *Chem. Phys. Lett. 232* (5−6), 429−436.

(23) Berger, O., Edholm, O., and Jahnig, F. (1997) Molecular dynamics simulations of a fluid bilayer of dipalmitoylphosphatidylcholine at full hydration, constant pressure, and constant temperature. *Biophys. J. 72* (5), 2002−2013.

(24) MacCallum, J. L., and Tieleman, D. P. (2006) Computer simulation of the distribution of hexane in a lipid bilayer: Spatially resolved free energy, entropy, and enthalpy profiles. *J. Am. Chem. Soc. 128* (1), 125−130.

(25) Anezo, C., de Vries, A. H., Holtje, H. D., Tieleman, D. P., and Marrink, S. J. (2003) Methodological issues in lipid bilayer simulations. *J. Phys. Chem. B 107* (35), 9424−9433.

(26) Werner, T., Morris, M. B., Dastmalchi, S., and Church, W. B. (2012) Structural modelling and dynamics of proteins for insights into drug interactions. *Adv. Drug Delivery Rev. 64* (4), 323−343.

(27) Nose, S. (1984) A Unified Formulation of the Constant Temperature Molecular-Dynamics Methods. *J. Chem. Phys. 81* (1), 511−519.

(28) Tamamura, H., Sugioka, M., Odagaki, Y., Omagari, A., Kan, Y., Oishi, S., Nakashima, H., Yamamoto, N., Peiper, S. C., Hamanaka, N., Otaka, A., and Fujii, N. (2001) Conformational study of a highly specific CXCR4 inhibitor, T140, disclosing the close proximity of its

DOI: 10.1021/bi501526s
Biochemistry 2015, 54, 1505−1515

intrinsic pharmacophores associated with strong anti-HIV activity. *Bioorg. Med. Chem. Lett. 11* (3), 359−362.
(29) Conner, M., Hawtin, S. R., Simms, J., Wootten, D., Lawson, Z., Conner, A. C., Parslow, R. A., and Wheatley, M. (2007) Systematic analysis of the entire second extracellular loop of the V(1a) vasopressin receptor: Key residues, conserved throughout a G-protein-coupled receptor family, identified. *J. Biol. Chem. 282* (24), 17405−17412.
(30) Kumar, S., and Nussinov, R. (2002) Relationship between ion pair geometries and electrostatic strengths in proteins. *Biophys. J. 83* (3), 1595−1612.
(31) Lee, K. K., Fitch, C. A., and Garcia-Moreno, E. B. (2002) Distance dependence and salt sensitivity of pairwise, Coulombic interactions in a protein. *Protein Sci. 11* (5), 1004−1016.
(32) Thiele, S., Mungalpara, J., Steen, A., Rosenkilde, M. M., and Vabeno, J. (2014) Determination of the binding mode for the cyclopentapeptide CXCR4 antagonist FC131 using a dual approach of ligand modifications and receptor mutagenesis. *Br. J. Pharmacol. 171*, 5313−5329.
(33) Gerlach, L. O., Skerlj, R. T., Bridger, G. J., and Schwartz, T. W. (2001) Molecular interactions of cyclam and bicyclam non-peptide antagonists with the CXCR4 chemokine receptor. *J. Biol. Chem. 276* (17), 14153−14160.
(34) Labrosse, B., Brelot, A., Heveker, N., Sol, N., Schols, D., De Clercq, E., and Alizon, M. (1998) Determinants for sensitivity of human immunodeficiency virus coreceptor CXCR4 to the bicyclam AMD3100. *J. Virol. 72* (8), 6381−6388.
(35) Yoshikawa, Y., Oishi, S., Kubo, T., Tanahara, N., Fujii, N., and Furuya, T. (2013) Optimized method of G-protein-coupled receptor homology modeling: Its application to the discovery of novel CXCR7 ligands. *J. Med. Chem. 56* (11), 4236−4251.
(36) Luker, K. E., Gupta, M., Steele, J. M., Foerster, B. R., and Luker, G. D. (2009) Imaging ligand-dependent activation of CXCR7. *Neoplasia 11* (10), 1022−1035.
(37) Kofuku, Y., Yoshiura, C., Ueda, T., Terasawa, H., Hirai, T., Tominaga, S., Hirose, M., Maeda, Y., Takahashi, H., Terashima, Y., Matsushima, K., and Shimada, I. (2009) Structural basis of the interaction between chemokine stromal cell-derived factor-1/CXCL12 and its G-protein-coupled receptor CXCR4. *J. Biol. Chem. 284* (50), 35240−35250.
(38) Venkatakrishnan, A. J., Deupi, X., Lebon, G., Tate, C. G., Schertler, G. F., and Babu, M. M. (2013) Molecular signatures of G-protein-coupled receptors. *Nature 494* (7436), 185−194.
(39) Levoye, A., Balabanian, K., Baleux, F., Bachelerie, F., and Lagane, B. (2009) CXCR7 heterodimerizes with CXCR4 and regulates CXCL12-mediated G protein signaling. *Blood 113* (24), 6085−6093.
(40) Odemis, V., Lipfert, J., Kraft, R., Hajek, P., Abraham, G., Hattermann, K., Mentlein, R., and Engele, J. (2012) The presumed atypical chemokine receptor CXCR7 signals through G(i/o) proteins in primary rodent astrocytes and human glioma cells. *Glia 60* (3), 372−381.
(41) Hoover, W. G. (1985) Canonical Dynamics: Equilibrium Phase-Space Distributions. *Phys. Rev. A 31* (3), 1695−1697.

DOI: 10.1021/bi501526s
Biochemistry 2015, 54, 1505−1515